

STOCHASTIC CHARACTERIZATION AND NONSTATIONARY  
SIMULATION OF EARTHQUAKE ACCELEROGRAMS

Ben Tilliouine (I)

João Azevedo (II)

Presenting Author: Ben Tilliouine

SUMMARY

A method is developed for simulation of artificial earthquakes. A physical spectrum is presented and its significance discussed for the characterization of nonstationarity in intensity and spectral content of earthquake processes. A procedure is developed to model the temporal variation of the ground motion frequency content, and a very efficient algorithm, based on the analytical signal concept, is proposed. Estimation of the window width in the time domain is shown to be closely linked to the frequency resolution and stability of the method. Simulated earthquakes, obtained from Western United States strong-motion accelerograms, show an excellent correlation in both time and frequency domains, demonstrating the powerfulness of the procedure.

INTRODUCTION

Earthquake loading is not periodic in nature, nor regular in shape, and is conditional on several random variables (hypocenter, seismic moment, attenuation, spectral peaks, duration, etc.), introducing extra uncertainty in the design process. Until more is known about source theory and wave-propagation-path characteristics, the engineer needs to carefully extrapolate from "assessable" earthquake characteristics from a given area. So, there should be a simulation method to stochastically generate a family of artificial earthquakes that, although different, have the same "signature" as the actual earthquake record.

This simulation may prove very useful, especially for the design of complex structures that are expected to have nonlinear behavior during seismic motion, allowing a statistical treatment of the response parameters.

The proposed procedure (Ref. 1) can be stated as follows:

- a) Direct problem: Develop a method for nonstationary characterization of earthquake accelerograms that can describe the time-varying nature of the mean square amplitudes and spectral content.
- b) Inverse problem: Recover the original accelerogram or a class of compatible time functions, given the solution for (a).

The generated ensemble of synthetic accelerograms should be consistent with:

- a) The average characteristics of past records.

---

(I) Ecole Polytechnique de Algiers, Algeria.

(II) Research Assistant, The John A. Blume Earthquake Engineering Center, Stanford University, Stanford, CA.

- b) The subjective judgement about possible ground motion characteristics, or the results of a seismic hazard analysis for the site of interest.

#### NONSTATIONARY CHARACTERIZATION OF EARTHQUAKE RECORDS

##### Proposed Model

Because the energy released at the source is finite, a rise and decay in amplitudes is typical in strong-motion accelerograms. Also because various seismic waves, or groups of waves, reach a certain site at different times, one can expect a temporal variation of the spectral content.

This time-varying nature of the amplitude and frequency content of an earthquake can be represented through what is called the Physical Spectrum (Ref. 2), which is defined as:

$$P_{XX}(f,t) = E[F_w^* \cdot F_w] \quad (1)$$

where  $E[ ]$  denotes expected value and

$$F_w(f,t) = \int_{-\infty}^{\infty} x(s) w(t-s) \exp[-2\pi ifs] ds \quad (2)$$

is the running Fourier transform with  $w(t-s)$  a selected time window function.

The Physical Spectrum represents, at time  $t$ , the average energy contribution of the harmonic  $f$ , and its volume, when plotted against the frequency-time plane, is associated with the total power of the earthquake.

The Physical Spectrum is also simply related to well-established potential destructiveness measures of earthquake motions, like the Arias intensity,  $A$ :

$$E[A] = \frac{2\pi}{g} \int_{-\infty}^{\infty} P_{XX}(f,t) df dt \quad (3)$$

or the mean square Housmer's intensity,  $H$ :

$$E[H] = \frac{21\pi}{g} \int_{-\infty}^{\infty} P_{XX}(f,t) df dt \quad (4)$$

##### Window Techniques and Parameter Values

Several window time functions can be used, but two comments can be made about its length ( $L$ ) apart from its shape:

- a) The larger the  $L$ , the higher the spectral resolution. A long window length leads to more details in the spectrum.
- b) The smaller the  $L$ , the better the accuracy on the spectral estimates. A short window length represents more stability because the smoothing is done for a large frequency range.

A trade-off between resolution and stability has to be made when choosing the window characteristics. This involves experience and judgement about the goals of the analysis.

To keep the distortion level as low as possible, the following guidelines are recommended:

- a) The window spectrum should have a high resolution in the central lobe.
- b) The window spectrum should have very small side lobes.

This implies the use of a broad data window function without discontinuity in its derivative.

Although there is no such thing as an optimal window, it follows from the results obtained that a Gaussian window leads to satisfactory results if care is taken in controlling the parameter  $\sigma$  related to the maximum value  $\omega(0)$  and the deviation  $D$  (half the distance between inflection points), where

$$\omega(t) = 2\sigma(2\pi)^{1/2} \exp[-(2\pi\sigma t)^2] \quad (5)$$

$$D = (2)^{1/2}/4\pi\sigma \quad (6)$$

$$\omega(0) = 2\sigma(2\pi)^{1/2} \quad (7)$$

and the Fourier transform of  $\omega(t)$

$$W(f) = (2)^{1/2} \exp[-f^2/4\pi\sigma^2] \quad (8)$$

Equation 8 points out that the smaller the value of  $\sigma$ , the narrower the frequency band width of  $\omega(t)$  and the more accurate the spectral decomposition of the signal. But this is equivalent to making  $D$  a very large value, which may cause an unrealistic local weighted average of the input data around time  $t$ .

#### Parameter Values for Nonstationary Simulation

To obtain  $x_m(t)$ , the  $m^{\text{th}}$  synthetic sample of the generated process, the Physical Spectrum values are evaluated at each time step  $\Delta t$ , the time spacing in the original record, and for each frequency  $f_k$ ,  $k = 1, 2, \dots, N$ , where  $N$  is the index associated with the highest frequency of interest and chosen to avoid aliasing effects.

For the filtered accelerogram band-width of 0.07-25 Hz and for  $\Delta t = 0.02$  sec, this corresponds to 25 Hz =  $1/2 \Delta t$  or  $N = 128$  spot frequencies ( $N$  is chosen to be a power of 2).

Also in this work the full deviation width is chosen to be equal to the full width associated with half the maximum value of  $\omega(t)$ ,

$$2D = N' \Delta t [2 \ln(2)]^{1/2} \quad (9)$$

where  $N'$  is the sample number defining the full width at half the maximum value of the window function.

With regard to the window length, the Gaussian window is truncated such that its tail amplitude is equal to  $1/\gamma$  of  $\omega(o)$ , resulting in a window length

$$L = 2D[2 \ln(\gamma)]^{1/2} \quad (10)$$

It was found that the values  $\gamma = \exp(2)$  and  $N' = 128$  which characterize the length and shape of the window function, respectively, were large enough to ensure a gradual tapering off towards both ends of the window length  $L$ .

However, the truncation requires that the spectrum of  $\omega(t)$ , as derived in Eq. 8 be corrected:

$$W'(f) = W(f) \operatorname{erf}(2\pi L\sigma) \quad (11)$$

or

$$W'(f) = W(f) \operatorname{erf}\{2[\ln \gamma]^{1/2}\}$$

As several Fourier transforms have to be computed to evaluate the Physical Spectrum, special techniques (Ref. 3) based on the concept of an analytical signal were used, allowing two real data streams to be transformed on one cell of a complex FFT routine, which represents a 45% improvement in program run time.

#### Nonstationary Analysis of Earthquake Records

The results of the nonstationary analysis of a few strong motion records are illustrated through various Physical Spectrum representations. Figures 1 and 2 show the spectrum values for two different waves, the 1.4 and 2.1 Hz components of the S00E component of the 1940 El Centro earthquake. Nonstationarity of both waves as well as smooth time variations are readily evident.

From these figures an interesting feature can be observed. The late arrival of a burst of energy associated with the 2.1 Hz component can in some cases be detrimental to structures which, due to the initial part of the motion, change their dynamic characteristics.

Figure 3 shows the Physical Spectrum for the above-mentioned accelerogram. The energy distribution in the frequency-time plane is well illustrated via this kind of representation. It evidences the multiple-rupture nature of the earthquake, as compared to impulsive earthquakes like the N65E component of 1966 Parkfield earthquake (Fig. 4).

#### Simulation of Earthquake Ground Motions

After obtaining the Physical Spectrum of an accelerogram, various artificial accelerograms can be simulated that are consistent with the time variation of the spectral content of the original signal. Of course, this family of accelerograms can also be generated based on an estimated Physical Spectrum, be it a smoothed average of a group of Physical Spectra from a set of accelerograms, or an idealized Physical Spectrum based on a prediction for an event with certain characteristics.

Let the  $m^{\text{th}}$  ensemble member of the process be

$$x^m(t) = \sum_{k=1}^N x_k^m(f_k, t) \quad (12)$$

where

$$x_k^m(f_k, t) = A(f_k, t) \sin(2\pi f_k t + \theta_k^m) \quad (13)$$

and  $\theta_k^m$  is the  $k^{\text{th}}$  sampled value of a random-phase angle  $\theta$  belonging to the  $m^{\text{th}}$  ensemble member, with uniform probability density function over the range  $-\pi \leq \theta \leq \pi$ .

Thus, if sets of independent random-phase angles are generated, and using the fact that the intensity envelopes  $A(f, t)$  are explicitly related to the Physical Spectrum, an ensemble of simulated ground motions can be generated with the same characteristics of the original or idealized one. Figures 5 and 6 show the previously mentioned El Centro accelerogram and a simulated accelerogram based on the obtained Physical Spectrum, respectively. More of these comparisons, as well as a more detailed look at the programs used in the analysis, can be found in Ref. 4.

#### CONCLUSIONS

The fact that the temporal and frequency nonstationarities are clearly visible with the notion of the Physical Spectrum, makes one think that:

- a) It is possible to reduce the uncertainty associated with the intensity characteristics at the focal mechanism and the attenuation parameters, if they are made frequency-dependent.
- b) It is possible to define a frequency-dependent PGA.
- c) It is possible to incorporate nonstationarity into earthquake design by studying the effect of the way peaks are distributed on time on the structural response. This will certainly be crucial for nonlinear behavior.
- d) It is possible to use an energy approach due to the fact that the Physical Spectrum is itself a time- and frequency-dependent energy input.

#### ACKNOWLEDGEMENTS

This work was performed while the first author was a Ph.D. student at Stanford University, under the supervision of Prof. H. C. Shah. The support from the Ministry of Education of Algeria and the John A. Blume Earthquake Engineering Center, Stanford University, Stanford, CA, is gratefully acknowledged.

#### REFERENCES

1. Tiliouine, B. (1982). "Nonstationary analysis and simulation of seismic signals," Ph.D. Dissertation, Civil Engineering Department, Stanford University, Stanford, CA.
2. Mark, W. D. (1970). "Spectral analysis of the convolution and filtering of nonstationary stochastic process," J. Sound and Vibrations, Vol. 11, No. 1.

3. Brigham, E. O. (1974). Fast Fourier Transform. Prentice-Hall, Inc., Englewood Cliffs, NJ.
4. Tiliouine, B., J. Azevedo, and H. Shah. "SIMUL--a computer program for stationary analysis and simulation of earthquake signals," Report to be published by the John A. Blume Earthquake Engineering Center, Stanford University, Stanford, CA.

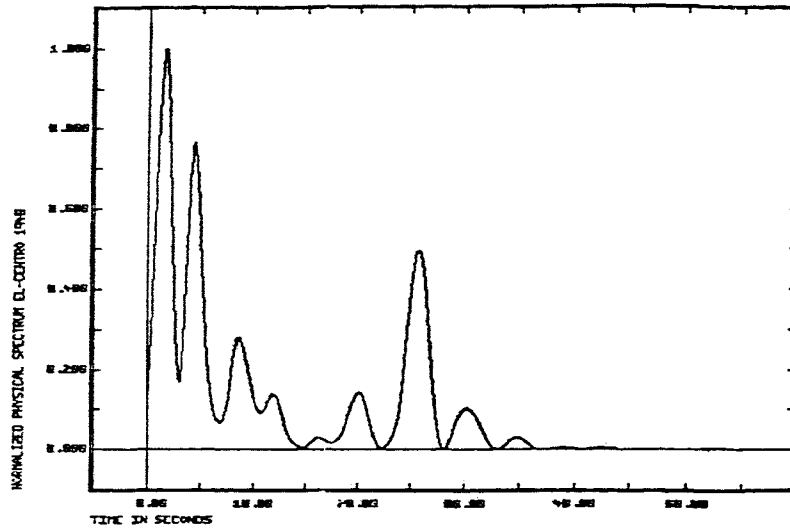


Figure 1. Physical spectrum - 2.1 Hz wave component.

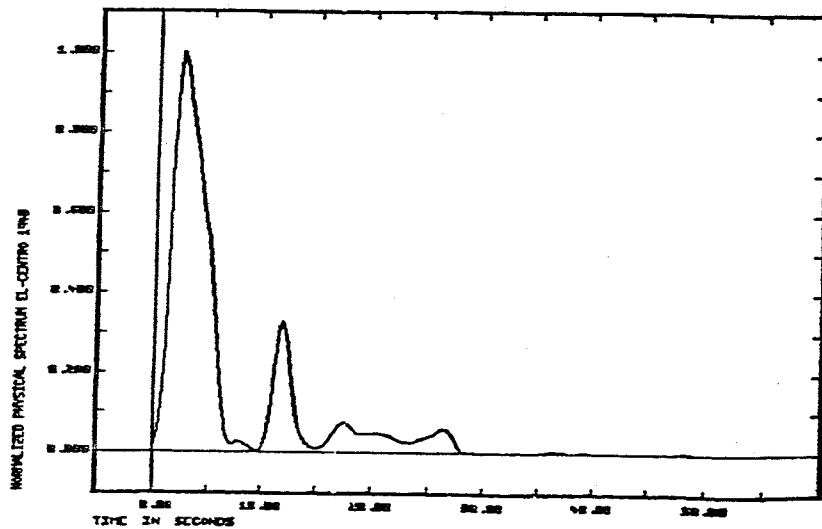


Figure 2. Physical spectrum - 1.4 Hz wave component.

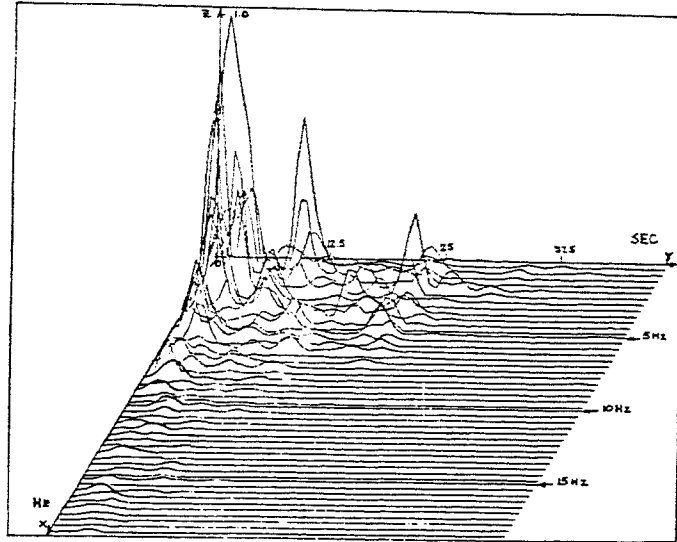


Figure 3. Physical spectrum - 1940 El Centro S00E.

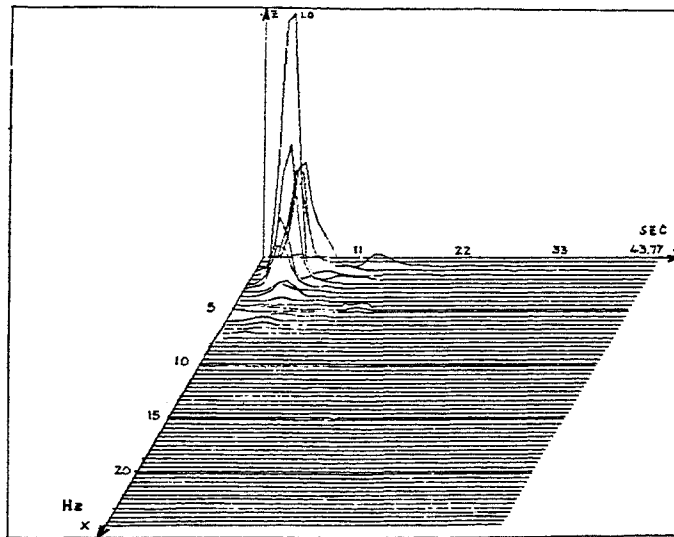


Figure 4. Physical spectrum - 1966 Parkfield N65E.

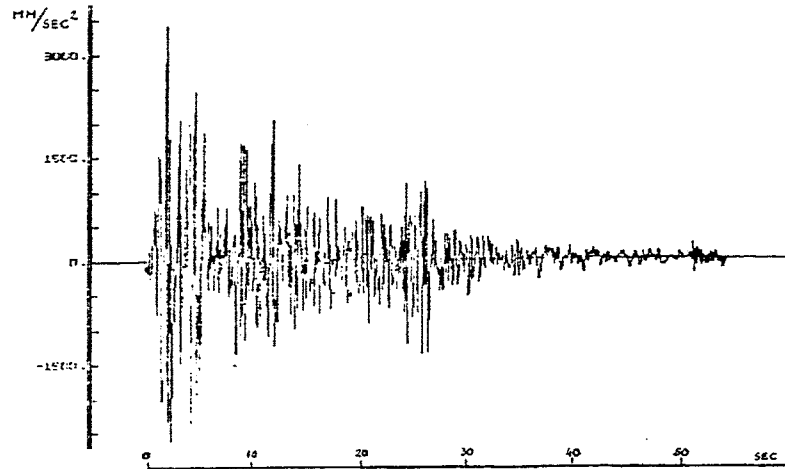


Figure 5. 1940 El Centro earthquake - S00E.

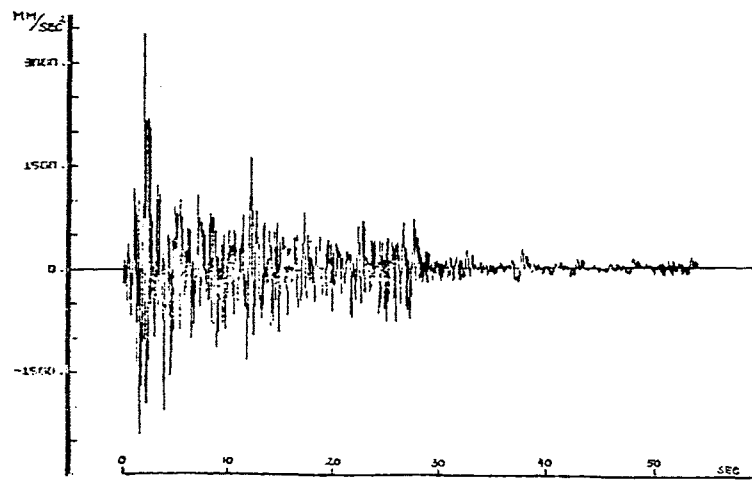


Figure 6. Simulated El Centro earthquake.